MOEMS for Space Applications: The Challenge of Multi-Wafer Bonding

Sylwester Bargiel, Frédéric Zamkotsian, Ludovic Gauthier-Manuel, Djaffar Balharet, Roland Salut

MOEMS for space applications: the challenge of multi-wafer bonding

Sylwester Bargiel
Université de Franche-Comté, CNRS,
Institut FEMTO-ST,
Besançon, FRANCE
sylwester.bargiel@femto-st.fr

Frederic Zamkotsian
Laboratoire d'Astrophysique de
Marseille (LAM), Aix Marseille Univ.,
CNRS, CNES,
Marseille, FRANCE
frederic.zamkotsian@lam.fr

Ludovic Gauthier-Manuel
Université de Franche-Comté, CNRS,
Institut FEMTO-ST,
Besançon, FRANCE
ludovic.gauthier@femto-st.fr

Djaffar Balharet
Université de Franche-Comté, CNRS,
Institut FEMTO-ST,
Besançon, FRANCE
djaffar.belharet@femto-st.fr

Roland Salut
Université de Franche-Comté, CNRS,
Institut FEMTO-ST,
Besançon, FRANCE
roland.salut@femto-st.fr

***Abstract*— MOEMS devices are key devices for next generation optical instruments, including space missions for Earth and Universe Observation. They will be used for object/wavelength selection and wavefront control. MIRA is a European development of micro-mirror arrays, with 100 x 200µm² silicon mirrors with remarkable surface quality and actual ability to work at cryogenic temperatures (162K). The challenge of multi-wafer bonding, especially on silicon micro-pillars is developed in this paper. Three bonding methods are proposed as well as various non-destructive and destructive methods of bonding characterisation. Low-temperature plasma-assisted Si-SiO_2 direct bonding is described in details as very promising method to obtain strong bond on micropillars.**

Keywords*— MOEMS, micro-mirror arrays, space instruments, Universe Observation, Earth Observation, wafer-level bonding

I. INTRODUCTION

Scientific return in next generation of space missions for Earth and Universe Observation will be upgraded using MOEMS devices. New generation of instruments could be designed with large micro-mirror arrays (MMA). In Universe Observation, the formation and evolution of galaxies are studied with multi-object spectrographs (MOS) in space and ground-based telescopes. A programmable slit mask for astronomical object selection is needed; 2D micro-mirror arrays are perfectly suited for this goal. In Earth Observation, the straylight in the spectrographs could be removed dynamically by using a Smart Slit, made of a 1D micro-mirror array as a gating device.

Multi-object spectroscopy (MOS) is one of the best tool for studying the formation and the evolution of galaxies with space and ground-based telescopes, especially for the measurement of infrared spectra of faint astronomical objects. A programmable slit mask for astronomical object selection is needed. MOEMS programmable slit masks could be used in future infrared MOS. We present in this paper the ability of a silicon-based micro-mirror array (MMA) to fulfil the performances requested by MOS instruments in space.

Three programmable slits devices are developed for new applications; two of them are studied by institutes and the last one is commercially available. The micro-shutter arrays (MSA) are developed by NASA to be mounted in the Near Infrared Spectrograph (NIRSpec) instrument in James Webb Space Telescope (JWST) [1]. NASA's Goddard Space Flight Center teams have designed, realized and characterized the MSA. The MSA uses a combination of magnetic actuation, and electrostatic latching of the shutters in the open position. The arrays have been tested at 30K and integrated in the instrument. JWST has been launched in 2021 and this device is the first MOEMS device fully operational in a space instrument. A European development of micro-mirror arrays for generating reflective slit masks has been initiated by Laboratoire d'Astrophysique de Marseille (LAM, France) together with Ecole Polytechnique Fédérale de Lausanne (EPFL, Switzerland) and Centre Suisse d'Electronique et de Microtechnologies (CSEM, Switzerland), in order to operate in future Multi-Object Spectrographs [2, 3]. The last device is a popular commercial array, the Digital Micromirror Device (DMD) from Texas Instruments (TI). This DMD has 2048 x 1080 mirrors with a 13.68µm pitch and has been tested for space applications [4].

II. MIRA PROJECT

FEMTO-ST and LAM are currently engaged in the project called **MIRA** for generating reflective slit masks in future MOS with micro-mirror arrays in Europe. The 100 x 200µm² micro-mirrors are electrostatically tilted, providing a precise actuated angle. The main requirements are cryogenic environment capabilities, uniform and precise tilt angle over the whole device, uniformity of the mirror voltage-tilt hysteresis and a very low mirror deformation.

The micro-mirror concept is based on the electrostatic double-plate actuator. A micro-mirror is suspended by two flexion hinges in polysilicon, which are attached to a sustaining frame (Fig. 1a). An electrode is located underneath the micro-mirror in order to generate an electrostatic force, and pillars are placed over the electrode plate to set a precise electrostatic gap between the micro-mirror and the electrode. A stopper beam is placed under the frame to set precisely the tilt angle of the micro-mirror after actuation. Finally, two landing beams are placed under each micro-mirror to avoid the micro-mirror to touch the electrode and generate short-circuits during the actuation.

When a voltage larger than the pull-in voltage is applied on the electrode, the micro-mirror is attracted by an electrostatic force towards the electrode. During this motion, it touches its stopper beam (Fig. 1b) and lands on its landing

pads. Therefore, the micro-mirror is electrostatically clamped at a precise tilt angle after pull-in (Fig. 1c).

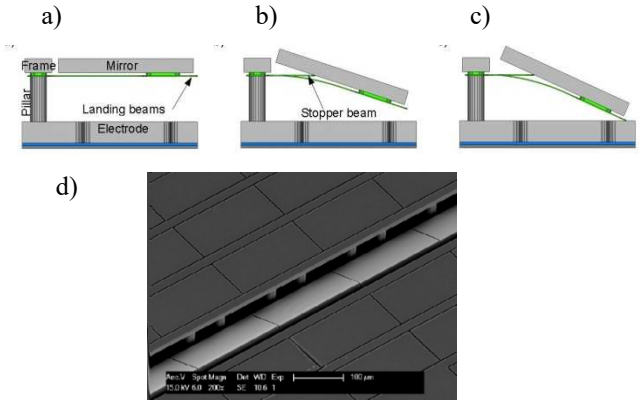

Fig. 1: MIRA device: a-c) Concept of a micro-mirror architecture and an electrostatic actuation scheme, d) SEM image of MMA with example of an actuation (line addressing mode).

When the voltage is decreased, the micro-mirror takes off from its stopper beam, and when the restoring force of the flexure beams is higher than the electrostatic force, the micro-mirror returns in its rest position. With an appropriate addressing mode, individual micro-mirror as well as a selected line of mirrors may be actuated (Fig. 1d).

III. Challenge of Multi-Wafer Bonding

Bulk and surface micromachining as well as wafer-level bonding are employed for the MMA microfabrication, using three wafers: two wafers for the mirrors (Si, SOI) and one for the electrodes (SOI). The wafers are processed separately and assembled by wafer-level bonding at the end of the process (Fig. 2). In order to increase the yield of the fabrication, the most critical step "electrode wafer to mirror wafer bonding" must be optimized.

A. Bonding requirements

The quality of multi-wafer bonding is a key factor to achieve operational MMA device, taking into account the challenging requirements of the space-oriented photonic application. For example, in order to allow operation in vacuum and at cryogenic temperatures, the device must be ideally mono-material with only Si-based structures. In practice, the number of construction materials is limited, mainly to Si, SiO_2 and polysilicon (poly-Si). The bonding method applied should not introduce other materials, especially those with very different thermal properties (CTE mismatch). It should not apply too high thermal treatment in the final assembly step to avoid damage or deformation of the poly-Si structures, ideally to be CMOS compatible (<450ºC). Hence, low-temperature direct bonding methods are preferable. Moreover, high bonding strength must be ensured for mechanical long-term stability and reliability of MMA device. Finally, the desired optical properties of the individual micro-mirrors (flatness, reflectivity, tilt angle) must be preserved during bonding process, indicating the condition of low level of residual stress in the bonded stack.

B. Current bonding achievements

Two different bonding steps were used in the previous fabrication process of MMA device: direct hydrophilic fusion Si-SiO_2 bonding and Au-Si eutectic bonding, as described in details in [3]. The first bonding step allowed the transfer of a 2µm-thick SiO_2 layer from an oxidized Si transfer wafer on top of the trenches of the mirror wafer (Fig. 2a). After prebonding in vacuum at room temperature, the fusion bonding was completed by annealing at 1050ºC for 3h. The transfer wafer was then completely etched by grinding and KOH etching. The poly-Si beams and the gold pads were then patterned on the mirror wafer. In the second bonding step, the mirror wafer was bonded by Au-Si eutectic bonding at 400ºC to the DRIE-processed electrode wafer with Si micropillars (Fig. 2b). Finally, the handle layer and the BOX of the mirror wafer were completely etched.

Although fabricated MMA device has exhibited very promising performances, some bonding-related issues were not fully resolved. The main problems identified, concerned the eutectic process – limited bonding strength on silicon micropillars and high residual stress in the multi-wafer stack. Indeed, as shown in Fig. 2c, the bonding must be performed on the array of tiny silicon micropillars, having the top surface (bonding pad) of only 9x22µm^2. This very small bonding area imposes challenging requirements on the bonding strength. While the Au-Si eutectic bonding is able to ensure such high strength, it suffers from residual stress due to local volumetric expansion, observed during the eutectic formation. Accumulation of the stresses, coming also from SOI wafers, resulted in often breakage of the micro-pillar bonding or the micro-mirror frame and, in consequence, low yield and degradation of actuation performances (higher operation voltage, incorrect tilt angle). As a consequence, an alternative bonding approach must be developed.

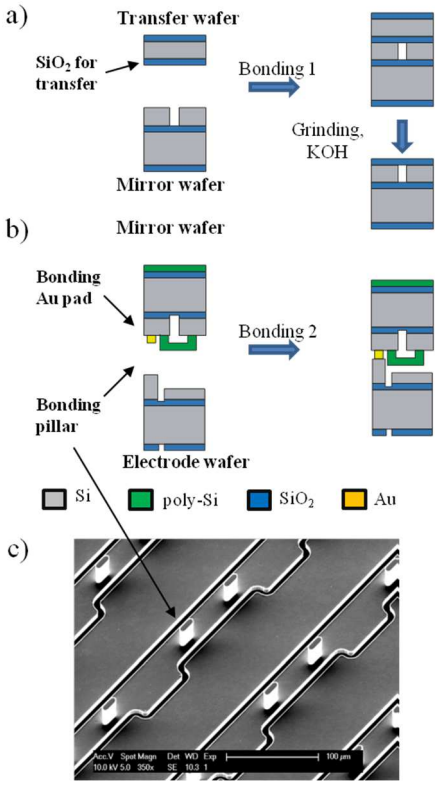

Fig. 2: Two key wafer-level bonding steps: a) Si-SiO_2 fusion bonding, b) Si-Au eutectic bonding, c) SEM image of array of Si micro-pillars on the electrode wafer.

IV. Alternative Bonding Techniques

Wafer-level bonding on large array of Si micro-pillars is a unique feature of the MMA fabrication process. The aim of this study is to select the best bonding method and to improve the bonding process towards the highest yield.

A. *Selection of bonding method*

Three alternative different bonding methods were proposed and tested in this work:

1) Silicon-GlassTF-Silicon anodic bonding (AB) through thin-film sodium-borosilicate glass layer was selected due to its relatively simple process flow and high strength, as demonstrated recently by Bargiel et al. for the fabrication of high-pressure micro-cooling devices [5]. A strong bond can be obtained at low bonding voltage (typ. 50-200V) and at medium temperature range (typ. 300-350°C), introducing lower residual stress when compared to standard AB process.

2) Room-temperature (RT) Si-Si direct bonding with fluorine containing plasma activation (O_2+CF_4) was also considered as very promising method, developed by Wang et al. [6]. High bonding strength, close to the bulk-fracture of Si, was reported without the use of neither wet chemistry nor annealing.

3) Direct plasma-assisted hydrophilic Si-SiO_2 bonding was also chosen since it offers high strength at much lower bonding temperature when compared to conventional fusion bonding (typ. 800-1000°C), without additional intermediate layers. This method benefits from conventional plasma activation step (typ. O_2, N_2) that increases the density of strong covalent Si-O-Si bonds at the interface at lower annealing temperature (typ. 200-450°C).

B. *Design and fabrication of test samples*

In order to test a wide range of bonding conditions, 26 different test structures (10 x 10mm^2) were designed. Each structure contains an array of micro-pillars, having the constant diameter (D = 10 - 100µm) and pitch (P= 25 - 400µm), surrounded by a 100µm wide frame. The test structures were distributed on the 4" wafer in such a way to obtain at least 2 structures of a given type as well as uniform density of bonding surface (total 72 structures per wafer). Electrode wafers with micropillars were fabricated on 500µm-thick, 4-inch DSP silicon substrates with TTV < 1µm. The wafers were selected in terms of low bow (7-15µm) and symmetrical 3D surface profile. Double-side photolithography and two DRIE Si etching processes were used to form ~30µm high micropillars on the top side and alignment marks for dicing on the bottom side (Fig. 3). Two versions of electrode wafer were fabricated, either with 1.0µm thermal SiO_2 layer or without it.

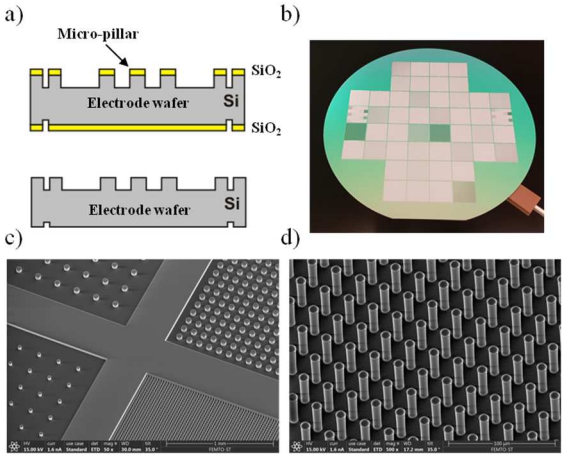

Fig. 3: Fabrication of test electrode wafer: a) two versions of the test structure with or without SiO_2 layer, b) wafer after DRIE etching of micropillar arrays, c) SEM image of various micropillar arrays, d) zoom on the smallest micropillars array (D/P=10/25µm).

V. BONDING TESTS

All bonding processes were carried out using AML AWB04 bonder (Applied Microengineering LtD, United Kingdom). This equipment allows "all-in-one" bonding approach where all key steps of a bonding process are performed in-situ, i.e. in the same vacuum chamber, including VIS/IR optical alignment of hot or cold wafers, surface plasma activation or vapour-based chemical treatment. These unique characteristics allow better control of surface preparation process in terms of cleanliness and state of the surface activation. Moreover, advanced control of bonding parameters as well as special side clamping system (no flags between bonded wafers) allow reliable process with lower stress. Bonding configurations used in the tests are presented schematically in Fig. 4.

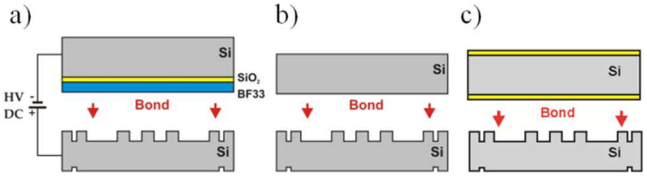

Fig. 4: Bonding configurations for three methods selected for tests: a) anodic bonding, b) RT direct Si-Si bonding, c) direct Si-SiO_2 bonding.

A. *Silicon-GlassTF-Silicon anodic bonding*

The electrode wafer was bonded to blank 4" Si wafer with deposited 1.0/4.0µm SiO_2/BF33 glass layers (Fig. 4a). According to the process, detailed in [5], the DC voltage was supposed to be applied progressively up to 150-180V, keeping the bonding current limited to 4mA. Although successfully tested on deeply structured Si wafers, this process turned out to be not adapted for micro-pillars due to very small bonding voltage (~35V), achieved during this test. The observed behaviour can be explained by too high electric field at the contact points between needle-like micro-pillars and deposited thin-film layers, resulting in a local electrical breakage. Additional chip-level bonding tests are in progress to determine the limit conditions on the micropillars.

B. *RT Si-Si direct bonding with fluorine containing plasma*

This bonding process relies on non-standard surface activation with precisely controlled content (~0.5%) of fluorine (CF_4) in the oxygen plasma. The main effort in this work was directed to establish optimal activation conditions, as found experimentally in [6], using available vacuum equipment and with related process limitations in terms of gas composition, flow rate and chamber pressure. RIE Corial machine was used for activation. Several Si-Si stacks were bonded in the configuration shown in Fig. 4b at different plasma conditions. They are under evaluation in terms of surface energy value. Ultimately, we would like to perform this activation process in the bonder chamber by injection of well-defined CF_4/O_2 mixture composition.

C. *Direct plasma-assisted hydrophilic Si-SiO_2 bonding*

The electrode wafer was bonded to blank 500µm-thick 4" Si wafer with TTV<1µm and 1.0µm thermal SiO_2 layer (Fig. 4c). Initially cleaned wafers undergone in-situ O_2/N_2 plasma activation, followed by a surface treatment with DI water vapour. Such prepared wafers were than pre-bonded in vacuum at room temperature, followed by low-temperature in-situ annealing (≤400°C). Several wafer stacks were successfully fabricated. The results of their characterization are presented in the next section.

VI. Characterisation of Bonded Structures

The wafer stacks, fabricated by direct Si-SiO_2 bonding method, were first analysed by several non-destructive (wafer level) methods to verify the stack deformation and general bonding quality (presence of contaminations, void density etc.). After dicing process, individual test structures were characterized in details by both non-destructive and destructive methods. We attempted to assess the effect of D/P parameters on the bonding yield which requires the quantification of the bonding related defects, and hence, the capacity to distinguish various type of potential defects at the micro-pillar bonding interface. The most demanding challenge was to obtain high-resolution images of the micro-pillars at the interface between two relatively thick Si wafers. Finally, harsh thermal fatigue tests in liquid nitrogen as well as destructive pull tests were also performed to verify the bonding strength.

A. 3D surface profile optical measurements

To verify the overall wafer-level deformation of the stack, an analysis of surface profile was performed with 3D surface interferometer (VerifireTM GPI XP interferometer, ZYGO). Low level of deformation in the bonded 4" wafer stacks was observed. A small values of peak-to-valley (P-V) profile amplitude were measured in the range of 10-15µm.

B. Wafer-level low-resolution IR imaging

Infrared inspection system, available in CL200 machine (Suss Microtec), revealed a bonding interface without visible big defects (e.g. trapped particles) and rarely with individual voids at the edge, as shown in Fig. 5a. Because of the limited optical resolution, individual micro-pillars were not visible.

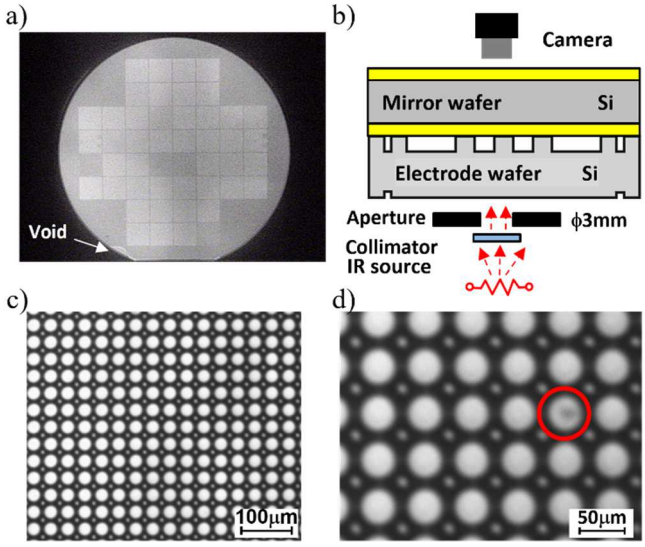

Fig. 5: Characterization of direct bonded Si-SiO_2 structures by IR imaging: a) wafer-level low resolution inspection, b) schematic of high resolution IR setup, c) imaging of individual array of micropillars D/P=40/50µm, d) example of local defect on micropillar (digital zoom).

C. High-resolution IR imaging

IR alignment microscope of the AML bonder, equipped with VIS/IR-sensitive CMOS cameras and 4x lens (pixel size 4.8µm, FOV 1.53x1.23mm^2, res. ~1µm) was used to observe the micropillar bonding interface. Individual micro-pillars with diameter exceeding D>20µm could be successfully observed, showing in general low density of local defects, i.e. a few in the FOV (Fig. 5c). However, the type of observed defects could not be identified in this optical setup as not sensitive to presence of a small gap at interface. Hence, it was not possible to distinguish bonded from unbonded micropillars. Moreover, as shown in Fig. 5d, it was also hard to distinguish the DRIE-related defects, such as locally damaged micropillar surface (hole), from bonding-related issues like the presence of a small particle on pillar.

D. High-resolution scanning acoustic microscopy SAM

A complementary inspection of the bonding interface was made by high-resolution acoustic imaging system (SAM302 HD^2, PVA TEPLA) since SAM exhibits high sensitivity to any gap, delamination, cracks etc. Transmission mode turned out to be not suitable for the micro-pillars imaging because of very low signal detected. Therefore, imaging was performed in reflective mode, in full immersion of the wafer stack in the water. The 150MHz transducer (f5.9mm) was chosen as a compromise between penetration depth and imaging resolution, resulting in ~15µm/pixel. Because of the big chip size, so-called HiSA scanning feature was employed to follow the local bow, and hence, to provide on the fly dynamic focus on the bonding interface. Although only bigger micropillars (D≥30µm) could be clearly observed, SAM imaging provided much more information allowing to distinguish DRIE-related defects from bonding-related ones (Fig. 6).

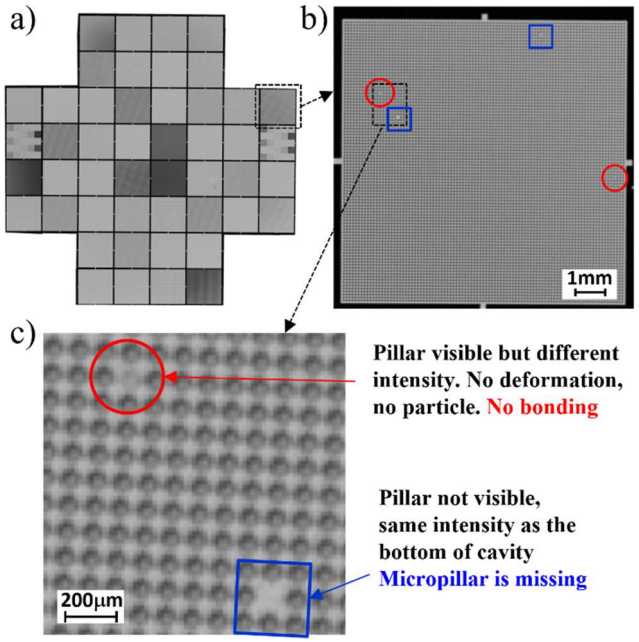

Fig. 6: Example of detailed SAM analysis: a) wafer scan, b) image of an individual array of micropillars (D/P=50/100µm), c) zoom on local defects.

E. Wafer dicing

The bonded wafer stack was successfully diced to obtain individual test structures (Fig. 7). Two methods were tested – standard diamond saw dicing and femto-second laser ablation. The saw dicing was performed in so-called polishing mode, which provides much lower sidewall roughness when compared to the laser machining. As a result, direct observation of bonding interface was possible. The successful saw dicing is considered as discriminative indicator of good bonding strength. Moreover, the detailed observation under SEM microscope revealed in some cases cracks at the micropillar base. Even with cracks due to the dicing process, the bonding interface did not show any visible deterioration, indicating strong bond.

F. Cryogenic tests

Four selected samples undergo thermal cycle, according to the scheme: RT > immersion in liquid nitrogen (-196°C) > natural heating to RT. All samples survived this harsh thermal loading without presenting any visible delamination or cracks.

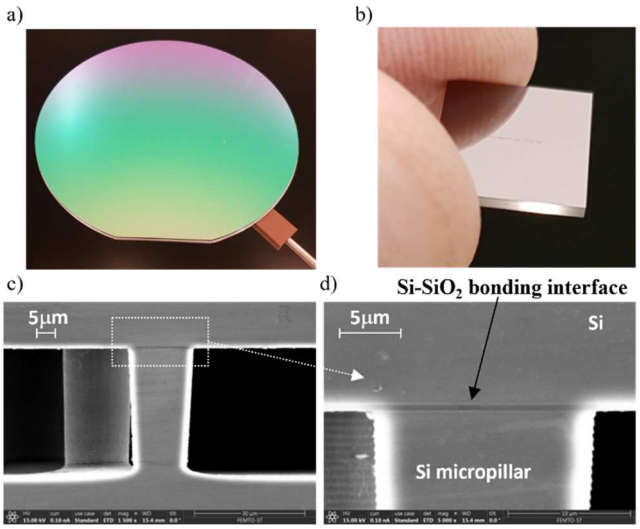

Fig. 7: Bonding inspection after saw dicing: a) photo of bonded stack (view on mirror wafer, b) individual 10x10mm^2 structure after dicing, c-d) SEM images of bonding interface.

G. Mechanical pull tests

Mechanical tests (pull mode) of selected structures were performed to determine the bonding strength. A microbond tester (DAGE Nordson 4000plus) was used in pull destructive mode. However, because of particular specificities of micropillar samples, the test methodology had to be modified in terms of mechanical configuration and the method of sample gluing. The pull tests are in progress to obtain reliable values.

VII. CONCLUSIONS, PERSPECTIVES

Development of reliable wafer-level bonding between two complex components of the MMA device (mirror and electrode wafers) is of great importance for the future of MIRA project. Bonding on large array of Si micro-pillars is a unique feature of the MMA fabrication process and it turns out to be the most challenging. Indeed, since each individual micromirror is supported by only two micropillars, bonding failure of only one micropillar results in failure or malfunction of the respective micromirror. This challenge will increase in the perspective of further miniaturisation of MMA device (smaller micro-mirror = smaller micropillars).

Three different methods of wafer-level bonding were foreseen for this purpose. At the current state of development, one method - low temperature plasma-assisted Si-SiO_2 bonding, was extensively tested and characterized using both non-destructive and destructive methods, showing very promising bonding performances. Nevertheless, the quantitative analysis of the bonding yield as a function of array D/P parameters was not yet achieved because of various limitations of the tested characterisation methods.

The high-resolution SAM method proved to be a powerful tool for micropillar bonding inspection. In the next characterisation phase, higher resolution SAM images are expected (~5µm/pixel) through an additional preamplifier and thinner Si layer. Practical inconvenience related to this improvement is much longer scanning time of the sample that remains fully submerged in the water. This may weaken in some cases the bonding energy, especially for low-temperature bonding processes, due to the water side penetration effect [7].

Although some local defects were still found at the micropillar bonding interface, as shown in Fig. 5 and Fig. 6, several improvements will be implemented in the next fabrication process. In order to reduce the DRIE-related defects (damaged micropillars), standard mask-based photolithography will be replaced by a direct writing photolithography. To decrease the risk of particle contamination, the SiO_2 layer stripping and wafer cleaning steps will be also optimized: the wet HF etching will be replaced by vapour HF method and additional DI-water magasonic rinsing/drying process will be added using CL200 (Suss Microtec) machine.

By increasing the yield of wafer-level bonding on micropillars, the critical process step of our micro-mirror array MIRA will be solved, allowing space applications of this device. They could be considered for future missions for Universe and Earth Observation.

ACKNOWLEDGMENTS

This work was financed by Actphast4R EU project in the frame of MIRA+ innovation project (P2021-43). The authors thank the French RENATECH network and its FEMTO-ST technological facility as well as Clara Haddad from MB Electronique for SAM imaging.

REFERENCES

[1] M. J. Li; A. D. Brown; A. S. Kutyrev; H. S. Moseley; V. Mikula, "JWST microshutter array system and beyond," Proc. SPIE 7594, San Francisco, USA (2010)

[2] S. Waldis, F. Zamkotsian, P.-A. Clerc, W. Noell, M. Zickar, N. De Rooij, "Arrays of high tilt-angle micromirrors for multiobject spectroscopy," IEEE Journal *of Selected Topics in Quantum Electronics* 13, pp. 168–176 (2007).

[3] M. Canonica, F. Zamkotsian, P. Lanzoni, W. Noell, N. de Rooij, "The two-dimensional array of 2048 tilting micromirrors for astronomical spectroscopy," Journal of Micromechanics and Microengineering, 23 055009, (2013)

[4] F. Zamkotsian, P. Lanzoni, E. Grassi, R. Barette, C. Fabron, K. Tangen, L. Valenziano, L. Marchand, L. Duvet "Successful evaluation for space applications of the 2048x1080 DMD" *Proc. of the SPIE conference on MOEMS*, Proc. SPIE 7932, San Francisco, USA (2011)

[5] S. Bargiel, J. Cogan, S. Queste, S. Oliveri, L. Gauthier-Manuel, M. Raschetti, O. Leroy, S. Beurthey and M. Perrin-Terrin, "Comparison of anodic and Au-Au thermocompression Si-wafer bonding methods for high-pressure microcooling devices", *Micromachines 2023*, 14, 1297, doi: 10.3390/mi14071297

[6] C. Wang, T. Suga, "Room-Temperature Direct Bonding Using Fluorine Containing Plasma Activation". *J. Electrochem. Soc.* 2011, *158*, H525, doi:10.1149/1.3560510.

[7] F. Rieutord, S. Tardif, D. Landru, O. Kononchuk, V. Larrey, H. Moriceau, M. Tedjini, F. Fournel, "Edge Water Penetration in Direct Bonding Interface", *ECS Transactions*, 2016. 75(9), 163–167. https://doi.org/10.1149/07509.0163ecst